



Spin polarized state filter based on semiconductor–dielectric–iron–semiconductor multi-nanolayer device



Vladimir I. Makarov^{a,*}, Igor Khmelinskii^b

^a Department of Physics, University of Puerto Rico, Rio Piedras, PO Box 23343, San Juan, PR 00931-3343, USA

^b Universidade do Algarve, FCT, DQF, and CIQA, 8005-139 Faro, Portugal

ARTICLE INFO

Article history:

Received 10 March 2014

Received in revised form 15 December 2014

Accepted 16 December 2014

Available online 17 December 2014

Keywords:

A. Interfaces

A. Magnetic materials

A. Semiconductor

B. Magnetic properties

D. Spin-density waves

ABSTRACT

Presently we report spin-polarized state transport in semiconductor–dielectric–iron–semiconductor (SDIS) four-nanolayer sandwich devices. The exchange-resonance spectra in such devices are quite specific, differing also from spectra observed earlier in other three-nanolayer devices. The theoretical model developed earlier is extended and used to interpret the available experimental results. A detailed *ab initio* analysis of the magnetic-field dependence of the output magnetic moment is also performed. The model predicts an exchange spectrum comprising a series of peaks, with the spectral structure determined by several factors, discussed in the paper.

Published by Elsevier Ltd.

1. Introduction

Various resonance phenomena are induced in a range of materials by continuous external microwave or radiofrequency electromagnetic fields in the presence of tunable magnetic fields and detected by steady-state resonance techniques or by pulsed microwave or radiofrequency fields in the presence of constant magnetic fields [1]. These include nuclear magnetic resonance, nuclear quadrupole resonance, ferromagnetic resonance, antiferromagnetic resonance, electron spin resonance, etc., observed in ferromagnetic and other materials. All of these resonance effects are strongly dependent on relaxation properties of spin states. The spin-lattice relaxation mechanisms have been studied earlier in detail for metals and metal particles of different size [2–9]. Spin-lattice relaxation in metals may be caused by (i) interaction of spin polarized states with electromagnetic fields induced by fluctuations of electric charge density, and (ii) phonon density, by (iii) SO interactions and (iv) higher-order interactions involving nuclear spin. The spin–spin relaxation processes also affect the spin state dynamics. Therefore, it is very important to develop new methods of theoretical and experimental studies of spin state dynamics in solid samples. The analysis of spin-polarized state dynamics using novel experimental and theoretical approaches is an important fundamental problem. The quantum spin-polarized state filter

(QSPSF) device described earlier for metal–dielectric–iron and metal–dielectric–semiconductor devices [10] allows to transfer spin-polarized states between nanolayers of different nature and chemical composition, and measure values of *g*-factor difference between nanolayers and the respective relaxation parameters of the spin-polarized states. Simple interpretations for the formation of spin-polarized states in ferromagnetics, conductors and semiconductors were analyzed [10]. A phenomenological model of spin-polarized state transfer was proposed and discussed [10]. This modeling approach assumes transfer of spin-polarized states between different nanolayers [10]. Experimental measurements of the exchange-resonance spectra in four-layer sandwich structures were also carried out [10]. The presently discussed semiconductor–dielectric–iron–semiconductor (SDIS) structures produce distinct spectra, differing from those obtained earlier for other nanolayer sandwich structures [10]. These spectra are analyzed and interpreted using the earlier and presently developed theoretical models.

2. Experimental

2.1. Device description

The experimental setup used in the current studies has already been described in detail [10]. It was built around the home-made nanosandwich device. This device included a ferrite needle (1) (TPS&TPSA, Power Electronics Technology), with the needle tip 50 μm in diameter made of a stainless-steel capillary filled with

* Corresponding author. Tel.: +1 787 529 2010; fax: +1 787 756 7717.
E-mail address: vmvimakarov@gmail.com (V.I. Makarov).

ferrite powder suspended in glycerol, and the body 1 mm in diameter. The saturation field and the frequency band for the ferrite are 11–13 kG and $\nu_{H,0} = (1 - 1.5) \times 10^8$ Hz, respectively. The transmission of the ferrite at frequencies $\nu_H > \nu_{H,0}$ is described by

$$\vartheta(\nu_H) = \vartheta(\nu_{H,0})e^{-\nu_H - \nu_{H,0}/\nu_{H,0}} \quad (1)$$

A spiral coil of copper wire (0.3 mm wire diameter, 10 turns) was wound on the needle body. The needle tip touched the surface of a Si substrate at the (100) plane. The opposite surface of the Si substrate, equally (100), was covered by a sandwich structure, prepared as described separately. A second ferrite item (TPS&TPSA, Power Electronics Technology), with the input surface 10 mm in diameter and the body 1 mm in diameter, contacted the output metal surface by way of a magnetic contact provided by ferrite powder suspended in glycerol (1:1 w/w) (TPS&TPSA, Power Electronics Technology, 25 μ m average particle diameter). Copper wire, 0.3 mm in diameter, was wound on the body of the item (10 turns). Note that the same high-frequency ferrite material was used everywhere, rated for up to 100 MHz applications. The entire assembly with the nanosandwich sample was placed into a liquid nitrogen bath ($T \approx 77$ K), to reduce noise.

The home-built current generator was controlled via an I/O data acquisition board (PCI-6034E DAQ, National Instruments), which was programmed in the LABVIEW environment that ran on a Dell PC. The generator fed pulsed currents of up to 10 A into the input coil. The pulse shape was programmed to reproduce the linear function:

$$I_2(t) = \begin{cases} 0, & 0 \leq t < t_0 \\ I_0 \times (t - t_0), & t_0 \leq t < t_0 + \tau \\ 0, & t_0 + \tau \leq t \end{cases} \quad (2)$$

where I_0 , t_0 and τ (pulse amplitude, start time and duration) were chosen to obtain the required magnetic field sweep rate. The output coil was connected to a digital oscilloscope (LeCroy; WaveSurfer 432), which collected and averaged the output signal. The I/O DAQ board generated an analog signal that controlled the current generator, and a rectangular TTL pulse 100 ns in duration that triggered the oscilloscope with its rising edge, 100 ns before the start of the analog control signal sweep.

2.2. Multilayer sandwich structure preparation

A detailed description of the device preparation procedure and multilayer sample characterization has been presented earlier [10]. Charge sputtering, vacuum evaporation and laser vapor deposition were used to deposit Fe, SnO_2 and Si, and SiO_2 layers, respectively. The nanolayer deposition procedure has been described earlier [10–12]. The layer thickness was controlled by transmission electron microscopy (TEM) on cross-cut samples, prepared using heavy-ion milling. A typical TEM image of SnO_2 ($h_{\text{SnO}_2} = 8.0$ nm)– SiO_2 ($h_{\text{SiO}_2} = 8.1$ nm)–Fe ($h_{\text{Fe}} = 7.9$ nm)–Si ($h_{\text{Si}} = 8.4$ nm) device is shown in Fig. 1. The four-nanolayer devices were used in the present series of experiments, with the measurements mostly conducted at LN₂ temperature (~ 77 K).

The exchange resonance spectra and their amplitude dependence on the magnetic field sweep rates were recorded using the same data acquisition system as earlier [10], briefly described above.

3. Results and discussion

We studied the exchange-resonance spectra for a series of four-nanolayer sandwich devices, with semiconductor–dielectric–iron–semiconductor (SDIS) structure. These SDIS devices used the SnO_2 ($h_{\text{SnO}_2} = 8.0$ nm), SiO_2 ($h_{\text{SiO}_2} = 8.1$ nm), Fe ($h_{\text{Fe}} = 7.9$ nm) and Si ($h_{\text{Si}} = 8.4$, 9.1, 9.7, 10.1, 10.8, 11.6, 12.3, 12.8, 13.5 and 14.1 nm) layers, with h_i

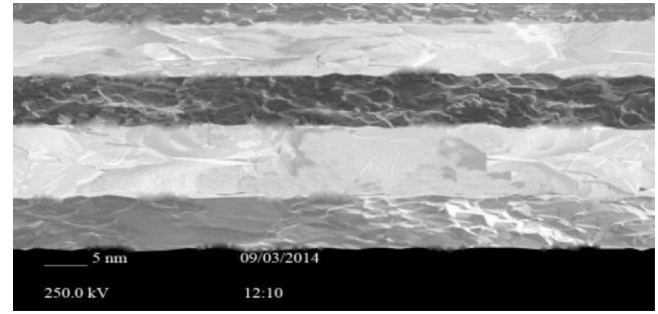


Fig. 1. TEM image of a cross-cut SnO_2 ($h_{\text{SnO}_2} = 8.0$ nm) + SiO_2 ($h_{\text{SiO}_2} = 8.1$ nm) + Fe ($h_{\text{Fe}} = 7.9$ nm) + Si ($h_{\text{Si}} = 8.4$ nm) sandwich structure on a Si substrate.

denoting the respective layer thickness. All of these devices were tested at LN₂ temperatures, using a 50 μ m diameter needle tip. The magnetic field sweep rate was 0.684 kG/ μ s, with the maximum magnetic field of 6.84 kG generated at 10 μ s sweep duration. Fig. 2 shows typical experimental exchange resonance spectra obtained presently.

Fig. 2a demonstrates the complete exchange resonance spectrum recorded within the total sweep range of 0 to 10 μ s, while Fig. 2b shows only the lower-field part of the same spectrum recorded at shorter sweep times. Detailed analysis suggests that the spectra may be represented by a superposition of at least four independent spectral components, shown in Fig. 3. These components were extracted as described below.

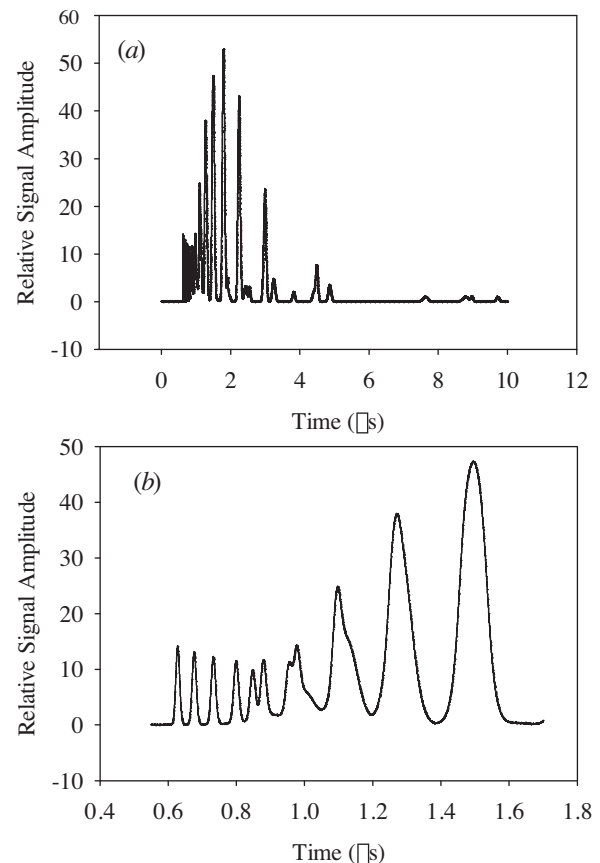


Fig. 2. Output signals of a four-layer (a) SnO_2 ($h_{\text{SnO}_2} = 8.0$ nm), SiO_2 ($h_{\text{SiO}_2} = 8.1$ nm), Fe ($h_{\text{Fe}} = 7.9$ nm) and Si ($h_{\text{Si}} = 8.4$ nm) device presented on the entire available time scale, (b) initial part of the spectrum of (a). The data were recorded at 77 K.

Download English Version:

<https://daneshyari.com/en/article/1487581>

Download Persian Version:

<https://daneshyari.com/article/1487581>

[Daneshyari.com](https://daneshyari.com)